ScientificScholar®
Knowledge is power
Publisher of Scientific Journals

www.surgicalneurologyint.com

Surgical Neurology International

Editor-in-Chief: Nancy E. Epstein, MD, Professor of Clinical Neurosurgery, School of Medicine, State U. of NY at Stony Brook.

SNI: Neurovascular

Editor
Kazuhiro Hongo, MD
Shinshu University, Matsumoto, Japan

SNI
Open Access

Original Article

Inter-modality correlation across invasive and non-invasive angiography in the three-dimensional assessment of cerebral aneurysms

Mark D. Johnson, Seth Street, Charles J. Prestigiacomo

Department of Neurosurgery, University of Cincinnati, Cincinnati, Ohio, United States.

E-mail: *Mark D. Johnson - johns5m5@ucmail.uc.edu, Seth Street - streetss@mail.uc.edu; Charles J. Prestigiacomo - presticj@ucmail.uc.edu

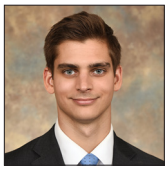

***Corresponding author:**
Mark D. Johnson,
Department of Neurosurgery,
University of Cincinnati,
Cincinnati, Ohio, United States.

johns5m5@ucmail.uc.edu

Received: 28 November 2024
Accepted: 08 January 2025
Published: 14 February 2025

DOI
10.25259/SNI_1019_2024

Quick Response Code:

ABSTRACT

Background: Non-invasive and invasive methods of cerebral angiography, including computed tomography angiography (CTA), magnetic resonance angiography (MRA), and digital subtraction angiography (DSA), are commonly used to characterize and follow cerebral aneurysms. Prior work has validated two-dimensional size measurements across these modalities. Our study aims to compare the reliability of three-dimensional (3D) shape measurements across CTA, MRA, and DSA.

Methods: A subset of cerebral aneurysms in which more than one form of angiography was performed was selected. Aneurysms were included if they did not change in size or shape between angiographic studies. Aneurysm domes were segmented, and morphometric features were measured consistent with prior reports. Intraclass correlation coefficients (ICCs) for each morphometric measure were calculated using a two-way mixed effect model.

Results: A total of 65 individual aneurysms from 55 patients were included in the study. The majority of aneurysms were imaged with DSA and CTA (43%) or MRA and CTA (40%), with 14% having DSA, MRA, and CTA available for review. The majority of aneurysms were located in the anterior circulation (77%), with an average size was 5 (4–8) mm. ICC ranged from 0.66 to 0.99 for 3D morphometric features, corresponding to "moderate" to "excellent" correlation. Sphericity and non-sphericity index showed the lowest ICC values. With the exception of these two variables, 3D morphometrics showed "good" or "excellent" reliability. No significant difference in mean absolute difference was noted across imaging modalities for each morphometric feature.

Conclusion: The majority of 3D morphometric measures show "good" to "excellent" reliability across CTA, MRA, and DSA, allowing for comparison across imaging modalities.

Keywords: Aneurysm, Angiography, Irregular, Morphology, Shape

INTRODUCTION

Until the 1990s, cerebral vascular imaging was limited to two-dimensional (2D) images from catheter-based angiography. In 1990, technical advances allowed for the identification of cerebral aneurysms with magnetic resonance angiography (MRA) with similar accuracy, and computed tomography angiography (CTA) became available in 1995.[4,29] The 1990s also set the stage for three-dimensional (3D) modeling of cerebral aneurysms, culminating in the introduction of

3D digital subtraction angiography (DSA) in 1997.[7,13,23] In clinical practice, both non-invasive (MRA/CTA) and invasive (DSA) methods of cerebral angiography are utilized to evaluate cerebral aneurysms.

In parallel to these advancements in imaging, links between aneurysm size, location, and rupture risk were described.[15,18,31] However, practical observations have shown that size alone is not a complete indicator of risk, as many ruptured aneurysms are relatively small, under 7 mm.[6,16] To gain a more holistic representation of an aneurysm's morphology, shape ratios, including the size, area, and aspect ratios (AR), have been investigated with variable results.[20,24] With continued advances in imaging and computing technology, the concept of describing 3D shape properties, or 3D morphometrics, of a cerebral aneurysm has been explored.[11] These 3D morphometrics show promise as objective measures of "irregularity," another feature consistently linked to aneurysm rupture status and classically, subjectively described.[10,25,27] Prior work has validated 2D size measurements across these various angiographic modalities; however, there is limited data on the reliability of 3D measurements across angiographic modalities.[1,17,19] Our study aims to compare the reliability of 3D shape measurements across CTA, MRA, and DSA.

MATERIALS AND METHODS

Selection of subjects

Retrospective data from our institutional registry of patients with ruptured and unruptured cerebral aneurysms over 8 years between January 1, 2014, and February 16, 2022, was reviewed for patients in which more than one form of cerebral angiography was performed and available for review. Aneurysms were included if they had a saccular morphology and did not change in size or shape by neuroradiologists or neuro interventionalists read between angiographic studies. CTA studies were completed on one of four General Electric (GE) Revolution Apex™ scanners at our institution. MRA studies were performed on either a GE SIGNA Artist Evo™ or a GE SIGNA Architect™ scanner at our institution. Syngo DynaCT images were collected during cerebral angiography on one of two Siemens Artis Zee Biplane machines.

The study protocol is consistent with the Strength in Reporting of Observational Studies in Epidemiology guideline. Our study received approval from our Institutional Review Board (IRB) under IRB #2019–1403, Department of Neurosurgery Retrospective Chart Review, with a waiver of the requirement to obtain informed consent since the research was determined to present less than minimal risk.

Segmentation and feature extraction

Aneurysm domes were manually segmented using the 3D slicer application (available at: https://www.slicer.org/).[5] The final segmentation for analysis was achieved by isolating each aneurysm from its parent vessel and slicing the segmentation directly across the ostium of the aneurysm. For CTA studies, the slice thickness varied between 0.5 and 1.25 mm, and pixel spacing varied between 0.39 and 0.55 mm. For MRA studies, the slice thickness varied between 1.20 and 1.60 mm, and pixel spacing varied between 0.42 and 0.60 mm. For DSA, the slice thickness was 0.5 mm, and pixel spacing was 0.22 mm.

The aneurysm segmentations were first rescaled to 0.48 × 0.48 × 0.48 mm voxel sizes to provide a consistent input for feature extraction. The slice thicknesses were normalized to this value to provide cubic voxels.

Two-dimensional (2D) measurements

2D measurements extracted included dome height (mm), neck width (mm), AR, surface area (SA), conicity parameter (CP), and bottleneck factor (BF). Dome height was measured as the maximal distance in millimeters perpendicular to the aneurysm ostium (neck plane). The neck width was measured as the maximal diameter in millimeters of the aneurysm ostium (neck plane). The AR was calculated consistent with prior descriptions as follows:[26]

$$AR = \frac{dome\,height\ (mm)}{neck\,width\ (mm)}$$

SA was automatically calculated within the Pyradiomics package within 3D Slicer (available at: https://pyradiomics.readthedocs.io/en/latest/installation.html) as follows:

$$A_i = \frac{1}{2}\left|a_i b_i \times a_i c_i\right| \quad (1)$$

$$SA = \sum_{i=1}^{N_f} A_i \quad (2)$$

Where the SA (A_i) of each triangle in the mesh is calculated, where a_ib_i and a_ic_i are edges of the i^{th} triangle in the mesh, formed by vertices a_i, b_i and c_i (1). Then, the total SA is then obtained by taking the sum of all calculated sub-areas (2).

CP was calculated as follows:[22]

$$CP = 0.5 - (height_{DMax}\ (mm)/dome\ height\ (mm)$$

Where $height_{DMax}$ is the height in millimeters of the maximal circumference of the aneurysm dome. BF was calculated as follows:[22]

$$BF = D_{max}/D_{neck}$$

Where D_{max} is the maximal circumference of the aneurysm dome perpendicular to the neck plane in millimeters, and D_{neck} is the circumference of the aneurysm ostium (neck plane) in millimeters.

Three-dimensional (3D) measurements

3D measurements extracted included the non-sphericity index (NSI), undulation index (UI), fractal dimension (FD), volume (V), elongation, flatness, and sphericity. NSI was calculated as follows:

$$NSI = 1 - \left(\frac{(18\pi)^{\frac{1}{3}} \times V^{\frac{2}{3}}}{SA}\right)$$

Where V is the volume of the mesh, and SA is its SA. SA to volume ratio was also calculated as the ratio between these two numbers. UI was calculated as follows:[22]

$$U1 = V/V_{CH}$$

Where V is the volume of the aneurysm mesh, and V_{CH} is the volume of the convex hull. The FD was calculated using a box-counting method utilizing an in house-built software previously described.[3] The general equation for the FD can be expressed as:

$$FD = \lim_{r \to o} \frac{\log N(r)}{\log r}$$

Where r is the box size, and N(r) is the number of cubes required to fill the shape. This calculation is estimated by performing a least squares regression to fit a line to a plot of log N(r) × log r, where the slope of the line is the FD. The Pyradiomics package within the 3D Slicer was utilized to calculate the volume, elongation, flatness, and sphericity.[5,28] Volume was calculated as follows:

$$V_i = \frac{Oa_i \times (Ob_i \times Oc_i)}{6} \quad \textbf{(1)}$$

$$V = \sum_{i=1}^{N_f} V_i \quad (2)$$

Where the volume of the region of interest (ROI) is calculated from the triangle mesh of the ROI for each face (i) in the mesh, defined by points a_i, bi, and c_i, volume of the tetrahedron defined by that face and the origin of the image (O) is calculated (1). Then taking the sum of all V_i, the total volume of the ROI is obtained (2). Elongation was calculated as follows:

$$elongation = \sqrt{\frac{\lambda_{minor}}{\lambda_{major}}}$$

Where λ_{major} and λ_{minor} are the lengths of the largest and second largest principal component axes. This feature is defined as the inverse of true elongation with values ranging between 1 (non-elongated) and 0 (maximally elongated). Flatness was calculated as follows:

$$flatness = \sqrt{\frac{\lambda_{least}}{\lambda_{major}}}$$

Where λ_{major} and λ_{least} are the lengths of the largest and smallest principal component axes. This feature is defined as the inverse of true flatness with values ranging between 1 (sphere-like) and 0 (a flat object). Sphericity was calculated as follows:

$$sphericity = \frac{\sqrt[3]{36\pi V^2}}{SA}$$

Where V is the volume, and SA is the SA. The value ranges between 0 (a flat object) and 1 (sphere-like). It is a dimensionless measure, independent of scale and orientation.

Statistical analysis

Data were presented as absolute values and percent totals for categorical variables and median ± 95% interquartile range for continuous variables. Intraclass correlation coefficients (ICCs) for each morphometric measure across imaging modalities were calculated using a two-way mixed effect model. The mixed effect model was chosen for this study as the imaging study modalities served as the "raters," generating the measurements and representing fixed effects when operated under the constraints of imaging acquisition protocols. The value of an ICC lies between 0 and 1, with 0 indicating no reliability among raters and 1 indicating perfect reliability. Interpretation of ICC values was in accordance with previously described thresholds where values <0.50 indicate "poor" reliability, values between 0.5 and 0.75 indicate "moderate" reliability, values between 0.75 and 0.9 indicate "good" reliability and values >0.9 indicate "excellent" reliability.[12] In addition, in the subset of aneurysms in which all three imaging modalities were available, we calculated the mean absolute difference for each morphometric feature across imaging modalities and compared these differences using an analysis of variance test. $P < 0.05$ was prospectively determined to be statistically significant. Analysis was performed using R version 3.6.0 (The R Foundation for Statistical Computing) and RStudio version 1.2.1335.

RESULTS

A total of 65 individual aneurysms from 55 patients had multiple forms of angiography available for review. Figure 1 illustrates the imaging modalities available for each aneurysm. The majority of aneurysms were imaged with DSA and CTA (43%) or MRA and CTA (40%), with 14% having DSA, MRA, and CTA available for

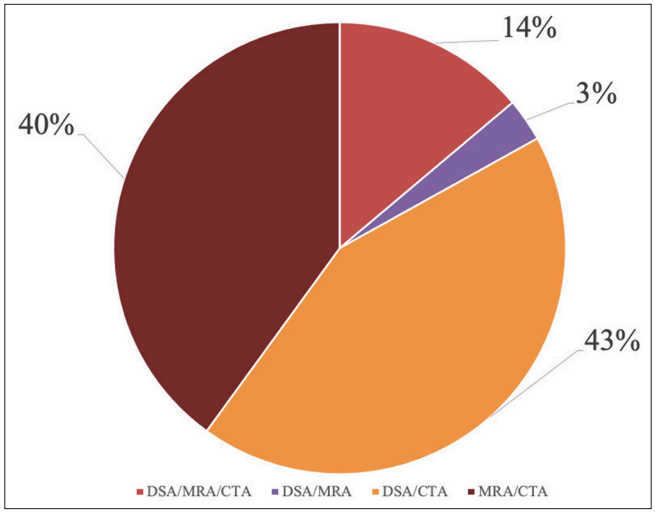

Figure 1: Proportion of patients with each combination of angiographic modalities available for review. DSA: Digital subtraction angiography, MRA: Magnetic resonance angiography, CTA: Computed tomography angiography,

review. Table 1 highlights the demographics of included patients and aneurysms. Female patients made up a large proportion of included patients (68%). The median size of included aneurysms was 5 (4–8) mm, with 43% classified as wide neck. Sidewall (48%) and bifurcation (52%) aneurysms were nearly equally represented. The majority of aneurysms were located in the anterior circulation (77%), with the anterior communicating artery (23% overall) and supra clinoid internal cerebral artery (32% overall) accounting for the most frequent locations.

ICC values for 2D morphometric and 3D morphometric features are shown in Table 2. For 2D morphometric features, ICC values ranged from 0.90 to 0.99, corresponding to "excellent" reliability. For 3D morphometric features, ICC values ranged from 0.66-0.98, corresponding to "moderate" to "excellent" reliability. Sphericity and NSI showed the lowest ICC values. With the exception of these two variables, 3D morphometrics showed "good" or "excellent" reliability. Volume showed the highest ICC for 3D morphometric features. The values for each aneurysm of the top four performing 3D morphometric features are shown in Figure 2. Close inspection of these plots highlights a trend toward closer grouping of measurements made on MRA and CTA for FD and volume compared to values obtained on DSA [Figure 2 panels a and b]. However, in the nine patients in which CTA, MRA, and DSA were available for review, the mean absolute difference for 2D and 3D morphometric features did not show a significant difference [Table 3].

Table 1: Demographic and aneurysm characteristics of included patients.

Demographics		***n*=65[1]**
Age (years)		63 (54, 67)
Female		44 (68)
Laterality		
	Right	26 (40)
	Left	17 (26)
	Midline	22 (34)
Anterior circulation		50 (77)
	AComm	15 (23)
	ICA	21 (32)
	ICA – Cavernous	3 (4.6)
	MCA	11 (17)
Posterior circulation		15 (23)
	PComm	3 (4.6)
	Basilar	7 (11)
	Vertebral artery	1 (1.5)
	PICA	1 (1.5)
	AICA	2 (3.1)
	SCA	0 (0)
	PCA	1 (1.5)
Size (mm)		5 (4, 8)
Wide neck[2]		28 (43)
Bifurcation		34 (52)
Sidewall		31 (48)
Irregular[3]		31 (48)

[1]N (%); Median (IQR), [2]≥4 mm or dome to neck ratio <2, [3]blebs, daughter sacs, or gross surface irregularity. AComm: Anterior communicating artery, ICA: Internal cerebral artery, ICA – Cavernous: Cavernous segment of the internal cerebral artery, MCA: Middle cerebral artery, PComm: Posterior communicating artery, PICA: Posterior inferior cerebellar artery, AICA: Anterior inferior cerebellar artery, SCA: Superior cerebellar artery, PCA: Posterior cerebral artery, IQR: Interquartile range

DISCUSSION

In a cohort of 65 individual aneurysms from 55 patients, we observed "moderate" to "excellent" reliability for the measurement of morphometric features across angiographic modalities. Our sample contained a wide variety of aneurysm locations that are consistent with prior reports on the natural prevalence.[9] The mean absolute difference for 2D and 3D morphometric features across modalities did not show a significant difference. Specifically looking at 3D morphometric features, sphericity and NSI showed the lowest ICC values. With the exception of these two variables, 3D morphometrics showed "good" or "excellent" reliability.

We were able to identify 65 total aneurysms in 55 patients followed at our institution over an 8-year period that was followed with multiple modalities of cerebral angiography and showed no shape or size change. The overall demographics of these patients and baseline characteristics of these aneurysms are generally reflective of the broad population with cerebral

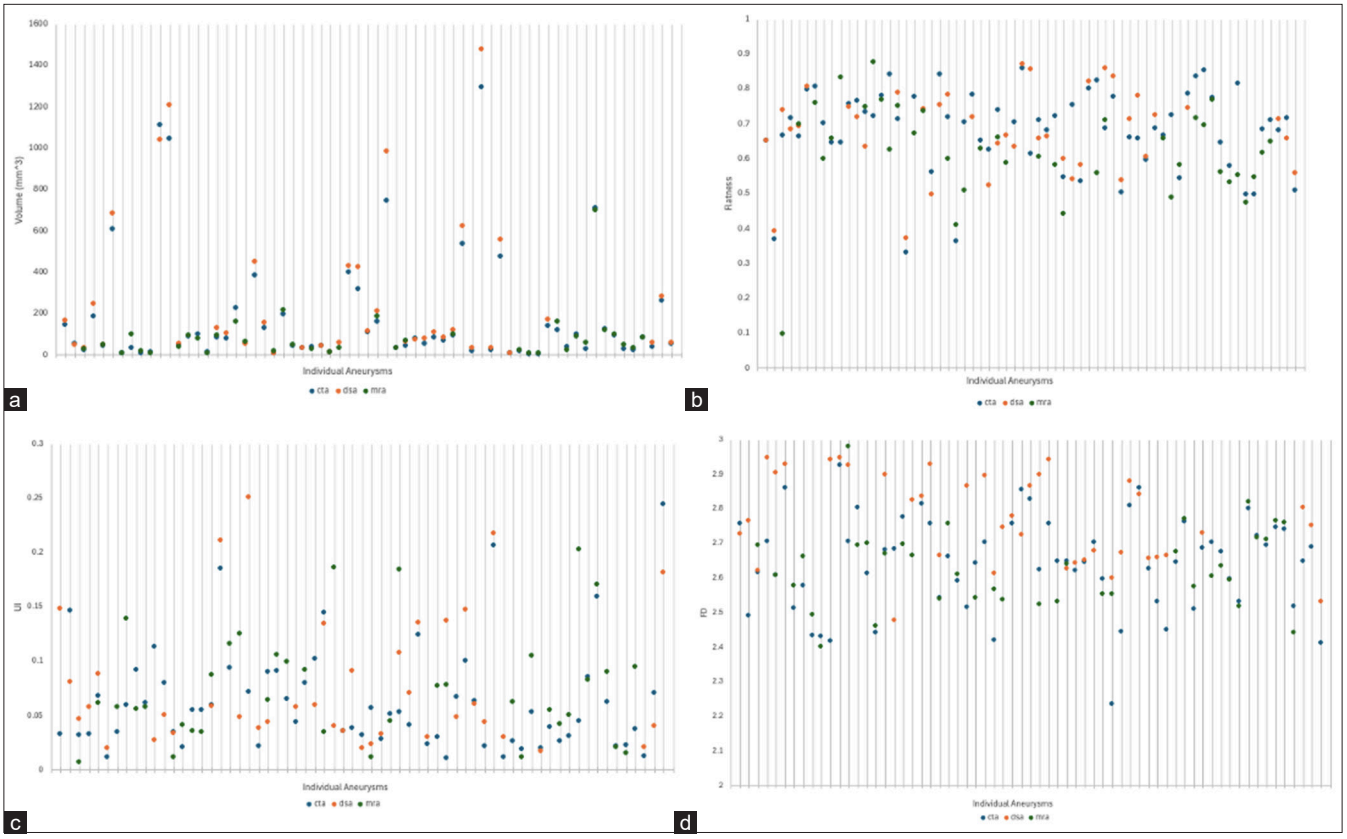

Figure 2: Plots of values obtained for (a) volume, (b) flatness, (c) undulation index (UI), and (d) fractal dimension (FD) obtained from the available angiographic modalities for each aneurysm highlighting the concordance of morphometric measurements between angiographic studies for each aneurysm. DSA:Digital subtraction angiography, MRA:Magnetic resonance angiography, CTA: Computed tomography angiography

aneurysms.[2,9,30] The distribution of aneurysm locations is also consistent with reports of location prevalence in larger populations adding to the generalizability of these observations.[2,9,30] We observed an interesting trend in study types obtained for each aneurysm. Nearly half of aneurysms were followed with non-invasive imaging modalities only, versus the other half receiving a DSA at some point. This may be a function of general clinical practice patterns as those aneurysms that were followed with only non-invasive imaging had an average size of <5 mm, while those with DSA performed at some time point averaged >8 mm in size.

We observed an overall "excellent" reliability for 2D features (ICC: 0.90–0.99) consistent with prior studies looking specifically at 2D measurements of cerebral aneurysms across imaging modalities.[1,17,19] An interesting observation in our data is an overall "excellent" agreement in neck width (ICC= 0.97) in our cohort. Previous reports have highlighted this measurement as showing the least reliability across imaging modalities and between individuals.[14,17] The high reliability observed in our study may be due to technical considerations in our imaging processing protocol. The neck widths were measured from the 3D meshes generated after standardizing the voxel sizes of each imaging modality, where prior studies obtained measurements without mention of standardization.[17] Given the impact neck width has on treatment decisions, significant work has gone into developing semi-automated and artificial intelligence-based algorithms for neck width measurements that now report rates of reliability across modalities similar to the results in our study.[8,21]

There have been limited reports on the reliability of 3D morphometric measurements across angiographic modalities to date, with several studies including volume in addition to 2D features.[19] The overall reliability for 3D morphometric features was lower than those observed with 2D features. This is not surprising as many of the 3D features quantify complex surface topography of the segmented aneurysm domes not captured with 2D measurements. Looking at the formulas for the two 3D measures that showed the lowest reliability, NSI and sphericity, we see that these measures share an almost identical formula with an inverse relationship. From a mathematical standpoint, NSI and sphericity are derived from SA and volume, compounding the measurement variabilities from these measures to the

Table 2: ICC values for 2D morphometric and 3D morphometric features.

	ICC	CI	Interpretation[1]
2D Features			
Dome height (mm)	0.99	0.98; 0.99	Excellent
Neck width (mm)	0.97	0.96; 0.98	Excellent
AR	0.95	0.92; 0.97	Excellent
SA	0.99	0.98; 0.99	Excellent
CP	0.97	0.95; 0.98	Excellent
BF	0.90	0.86; 0.94	Excellent
3D Features			
NSI	0.66	0.48; 0.78	Moderate
UI	0.77	0.65; 0.85	Good
FD	0.78	0.67; 0.86	Good
Volume	0.98	0.98; 0.99	Excellent
SA: V	0.99	0.98; 0.99	Excellent
Elongation	0.77	0.65; 0.85	Good
Flatness	0.78	0.66; 0.86	Good
Sphericity	0.71	0.57; 0.82	Moderate

[1]Definitions from Koo TK, Li MY. A Guideline of Selecting and Reporting Intraclass Correlation Coefficients for Reliability Research. *J Chiropr Med*. Jun 2016;15 (2):155-63. doi: 10.1016/j.jcm. 2016.02.012.
AR: Aspects ratio, SA: Surface area, CP: Conicity parameter, NSI: Non-sphericity index, UI: Undulation index, FD: Fractal dimension, SA: V: Surface area to volume ratio, BF: Bottleneck factor, ICC: Intraclass correlation coefficient, CI: Confidence interval

derived measures. One important consideration is that sphericity, a completely automated calculation, obtained a higher ICC value (0.71) than NSI (ICC: 0.66), a semi-automated calculation. With continued improvements in imaging resolution and artificial intelligence, we anticipate that the reliability of 3D morphometrics will continue to improve across study types.[21] As a proof of concept, the highest performing 3D morphometric features across modalities were volume, followed by FD, UI, and flatness, all of which are automated calculations from the raw 3D aneurysm meshes.

Our study is not without limitations. While the overall population demographics of our study are consistent with prior larger population level studies with regard to location and aneurysm size, we are limited by a relatively small number of included patients and aneurysms. We reviewed records over 8 years (the length of time our institution has utilized an electronic medical record) in an attempt to capture the maximum number of patients. One reason for the low number of eligible patients is the fact that many patients who were followed conservatively were routinely imaged with the same imaging modality across the follow-up period. This may be due to the exact clinical bias this work aims to challenge, in that aneurysm shape must be compared in an "apples to apples" manner with regard to angiographic imaging modality. Another limitation of this work is that the manual segmentation and measurement work was carried

Table 3: Mean absolute differences for 2D and 3D morphometric features in the subset of aneurysms with all three angiographic imaging modalities available for review.

	CTA versus MRA[1]	CTA versus DSA[1]	MRA versus DSA[1]	*P*-value
2D Features				
Dome height (mm)	0.4911	0.5530	0.5618	0.9398
Neck width (mm)	0.2768	0.3934	0.3965	0.6949
AR	0.1250	0.3042	0.2219	0.4123
SA	14.6544	24.3170	15.8872	0.3667
CP	0.0503	0.0197	0.0626	0.6173
BF	0.1107	0.1464	0.1502	0.8692
3D Features				
NSI	0.0290	0.0585	0.0414	0.1533
UI	0.0512	0.0342	0.0429	0.6371
FD	0.1043	0.1907	0.1395	0.3462
Volume	12.3959	18.3487	12.6590	0.6232
SA: V	0.1123	0.1302	0.1885	0.5304
Elongation	0.1270	0.0960	0.1322	0.8607
Flatness	0.1206	0.0796	0.1505	0.6170
Sphericity	0.0359	0.0737	0.0528	0.1439

[1]Mean absolute difference. AR: Aspects ratio, SA: Surface area, CP: Conicity parameter, NSI: Non-sphericity index, UI: Undulation index, FD: Fractal dimension, SA: V: Surface area to volume ratio, MRI: Magnetic resonance imaging, DSA: Digital subtraction angiography, BF: Bottleneck factor, CTA: Computed tomography angiography, MRA: Magnetic resonance angiography

out by one author, limiting our ability to assess the inter-rater reliability of measurements and the overall generalizability of our work.

CONCLUSION

Three-dimensional morphometric measures, with the exception of NSI and sphericity, for cerebral aneurysms on CTA, MRA, and DSA show "good" to "excellent" correlation across imaging modalities. With continued advancements in spatial resolution of angiography and improvements in automated imaging processing, we hope that this correlation will continue to improve. This data should provide reassurance to clinicians to make direct comparisons of these features across imaging modalities when obtained during follow-up. Additional studies may look at the cost-utility of specific angiographic modalities for follow-up and treatment planning.

Ethical approval: The research/study approved by the Institutional Review Board at the University of Cincinnati, number #2019–1403, dated 1/2019.
Declaration of patient consent: Patient's consent was not required as there are no patients in this study.
Financial support and sponsorship: Portions of this study were supported through grant funding from the Brain Aneurysm Foundation through the TeamCindy Chair of Research.
Conflicts of interest: There are no conflicts of interest.
Use of artificial intelligence (AI)-assisted technology for manuscript preparation: The authors confirm that there was no use of artificial intelligence (AI)-assisted technology for assisting in the writing or editing of the manuscript and no images were manipulated using AI.

REFERENCES

1. Abe Y, Yuki I, Otani K, Shoji T, Ishibashi T, Murayama Y. Agreement of intracranial vessel diameters measured on 2D and 3D digital subtraction angiography using an automatic windowing algorithm. J Neuroradiol 2021;48:311-5.
2. Agarwal N, Gala NB, Choudhry OJ, Assina R, Prestigiacomo CJ, Duffis EJ, *et al*. Prevalence of asymptomatic incidental aneurysms: A review of 2,685 computed tomographic angiograms. World Neurosurg 2014;82:1086-90.
3. Castiglione JA, Drake AW, Hussein AE, Johnson MD, Palmisciano P, Smith MS, *et al*. Complex morphological analysis of cerebral aneurysms through the novel use of fractal dimension as a predictor of rupture status. World Neurosurg 2023;175:e64-72.
4. Demaerel P, Marchal G, Casteels I, Wilms G, Bosmans H, Dralands G, *et al*. Intracavernous aneurysm. Superior demonstration by magnetic resonance angiography. Neuroradiology 1990;32:322-4.
5. Fedorov A, Beichel R, Kalpathy-Cramer J, Finet J, Fillion-Robin JC, Pujol S, *et al*. 3D Slicer as an image computing platform for the Quantitative Imaging Network. Magn Reson Imaging 2012;30:1323-41.
6. Forget TR Jr., Benitez R, Veznedaroglu E, Sharan A, Mitchell W, Silva M, *et al*. A review of size and location of ruptured intracranial aneurysms. Neurosurgery 2001;49:1322-5; discussion 1325-6.
7. Foutrakis GN, Burgreen G, Yonas H, Sclabassi RJ. Construction of 3-D arterial volume meshes from magnetic resonance angiography. Neurol Res 1996;18:354-60.
8. Groth M, Forkert ND, Buhk JH, Schoenfeld M, Goebell E, Fiehler J. Comparison of 3D computer-aided with manual cerebral aneurysm measurements in different imaging modalities. Neuroradiology 2013;55:171-8.
9. Hurford R, Taveira I, Kuker W, Rothwell PM, Oxford Vascular Study Phenotyped C. Prevalence, predictors and prognosis of incidental intracranial aneurysms in patients with suspected TIA and minor stroke: A population-based study and systematic review. J Neurol Neurosurg Psychiatry 2021;92:542-8.
10. Idil Soylu A, Uzunkaya F, Akan H. Anterior communicating artery aneurysms: Nonmodifiable morphological parameters associated with rupture risk. J Neuroimaging 2021;31:940-6.
11. Johnson MD, Palmisciano P, Yamani AS, Hoz SS, Prestigiacomo CJ. A systematic review and meta-analysis of 3-dimensional morphometric parameters for cerebral aneurysms. World Neurosurg 2024;183:214-26.e5.
12. Koo TK, Li MY. A Guideline of selecting and reporting intraclass correlation coefficients for reliability research. J Chiropr Med 2016;15:155-63.
13. Koyama T, Okudera H, Kobayashi S. Computer-assisted geometric design of cerebral aneurysms for surgical simulation. Neurosurgery 1995;36:541-6; discussion 546-7.
14. Maldaner N, Stienen MN, Bijlenga P, Croci D, Zumofen DW, Dalonzo D, *et al*. Interrater agreement in the radiologic characterization of ruptured intracranial aneurysms based on computed tomography angiography. World Neurosurg 2017;103:876-2.e1.
15. McCormick WF, Acosta-Rua GJ. The size of intracranial saccular aneurysms. An autopsy study. J Neurosurg 1970;33:422-7.
16. Mizoi K, Yoshimoto T, Nagamine Y. Types of unruptured cerebral aneurysms reviewed from operation video-recordings. Acta Neurochir (Wien) 1996;138:965-9.
17. Munarriz PM, Barcena E, Alen JF, Castano-Leon AM, Paredes I, Moreno-Gomez LM, *et al*. Reliability and accuracy assessment of morphometric measurements obtained with software for three-dimensional reconstruction of brain aneurysms relative to cerebral angiography measures. Interv Neuroradiol 2021;27:191-9.
18. Nehls DG, Flom RA, Carter LP, Spetzler RF. Multiple intracranial aneurysms: Determining the site of rupture. J Neurosurg 1985;63:342-8.
19. Nishi H, Cancelliere NM, Rustici A, Charbonnier G, Chan V, Spears J, *et al*. Deep learning-based cerebral aneurysm segmentation and morphological analysis with three-dimensional rotational angiography. J Neurointerv Surg 2024;16:197-203.
20. Parlea L, Fahrig R, Holdsworth DW, Lownie SP. An analysis of the geometry of saccular intracranial aneurysms. AJNR Am J Neuroradiol 1999;20:1079-89.

21. Planinc A, Spegel N, Podobnik Z, Sinigoj U, Skubic P, Choi JH, *et al*. Assessing accuracy and consistency in intracranial aneurysm sizing: Human expertise vs. artificial intelligence. Sci Rep 2024;14:16080.
22. Raghavan ML, Ma B, Harbaugh RE. Quantified aneurysm shape and rupture risk. J Neurosurg 2005;102:355-62.
23. Schueler BA, Sen A, Hsiung HH, Latchaw RE, Hu X. Three-dimensional vascular reconstruction with a clinical X-ray angiography system. Acad Radiol 1997;4:693-9.
24. Texakalidis P, Sweid A, Mouchtouris N, Peterson EC, Sioka C, Rangel-Castilla L, *et al*. Aneurysm formation, growth, and rupture: The biology and physics of cerebral aneurysms. World Neurosurg 2019;130:277-84.
25. UCAS Japan Investigators; Morita A, Kirino T, Hashi K, Aoki N, Fukuhara S, *et al*. The natural course of unruptured cerebral aneurysms in a Japanese cohort. N Engl J Med 2012;366:2474-82.
26. Ujiie H, Tachibana H, Hiramatsu O, Hazel AL, Matsumoto T, Ogasawara Y, *et al*. Effects of size and shape (aspect ratio) on the hemodynamics of saccular aneurysms: A possible index for surgical treatment of intracranial aneurysms. Neurosurgery 1999;45:119-29; discussion 129-30.
27. van der Kamp LT, Rinkel GJ, Verbaan D, van den Berg R, Vandertop WP, Murayama Y, *et al*. Risk of rupture after intracranial aneurysm growth. JAMA Neurol 2021;78:1228-35.
28. van Griethuysen JJ, Fedorov A, Parmar C, Hosny A, Aucoin N, Narayan V, *et al*. Computational radiomics system to decode the radiographic phenotype. Cancer Res 2017;77:e104-7.
29. Vieco PT, Shuman WP, Alsofrom GF, Gross CE. Detection of circle of Willis aneurysms in patients with acute subarachnoid hemorrhage: A comparison of CT angiography and digital subtraction angiography. AJR Am J Roentgenol 1995;165:425-30.
30. Vlak MH, Algra A, Brandenburg R, Rinkel GJ. Prevalence of unruptured intracranial aneurysms, with emphasis on sex, age, comorbidity, country, and time period: A systematic review and meta-analysis. Lancet Neurol 2011;10:626-36.
31. Wiebers DO, Whisnant JP, O'Fallon WM. The natural history of unruptured intracranial aneurysms. N Engl J Med 1981;304:696-8.

How to cite this article: Johnson MD, Street S, Prestigiacomo CJ. Inter-modality correlation across invasive and non-invasive angiography in the three-dimensional assessment of cerebral aneurysms. Surg Neurol Int. 2025;16:47. doi: 10.25259/SNI_1019_2024